THE PREPARATION AND CHARACTERIZATION OF THERMO-SENSITIVE COLORED HYDROGEL FILM AND SURFACTANT-FREE POROUS POLYSTYRENE THREE-DIMENSIONAL NETWORK

Bo Zhou, B.S

Thesis Prepared for the Degree of

MASTER OF SCIENCE

UNIVERSITY OF NORTH TEXAS

December 2001

APPROVED:

Zhibing Hu, Major Professor
William E. Acree Jr., Committee Member
Ruthanne D. Thomas, Chair of the Department of Chemistry
C. Neal Tate, Dean of the Robert B. Toulouse School of Graduate Studies

Zhour, Bo The preparation and characterization of thermo-sensitive colored hydrogel film and surfactant-free porous polystyrene three-dimensional network Master of Science (Chemistry), December 2001, 40 pp., 2 tables, 13 illustrations.

Polymer hydrogel films change their properties in response to environmental change. This remarkable phenomenon results in many potential applications of polymer hydrogel films. In this thesis colored thermo-sensitive poly(N-isopropylacrylamide) (PNIPAAm) hydrogel film was prepared by firstly synthesizing polymer latex and secondarily crosslinking the nanoparticles and casting the polymers onto glass. The shape-memory effect has been observed when changing the environmental temperature. The temperature-dependent of turbidity of polymer hydrogel film was measured by HP UV-Visible spectrophotometer. This intelligent hydrogel might be used in chemomechanical systems and separation devices as well as sensors.

Polymer adsorption plays an important role in many products and processes. In this thesis, surfactant-free three-dimensional polystyrene (PS) nanoparticle network has been prepared. The infrared spectroscopy and solubility experiment are performed to prove the crosslinking mechanism, also the BET method was used to measure the adsorption and desorption of polystyrene network. The BET constant (C) is calculated (C=6.32). The chemically bonded polymer nanoparticle network might have potential applications as catalyst or used for chromatographic columns.

ACKNOWLEDGEMENT

I wish to thank my major advisor Dr. Zhibing Hu for his enthusiastic guidance and friendly encouragement. His hard-working spirit impressed and stimulated me all the time. His many unique ideas benefit all his students a lot, additionally he is such a nice person that working with him is really a pleasure.

I also thanks for the help of Dr. Jun Gao (Postdoctoral, Department of Physics), Zhiling Zhang (Ph.D. Department of Biology) and Hanjiang Dong (Ph.D. Department of Material Science). Without their warm-hearted favor I cannot finish my project so fluently.

I also thank for Dr. Acree who give my thesis a careful reading and I am very appreciated for his suggestions.

Last but not the least, I want to give my thanks to my wife, Yinghua Wang. Her encouragement and care contributed a lot from the beginning to the finishing of this thesis.

TABLE OF CONTENTS

LIST OF TABLES

Table Page

LIST OF ILLUSTRATIONS

CHAPTER 1

SYNTHESIS AND CHARCTERIZATION OF THERMO-SENSITIVE COLORED HYDROGEL FILM

1.1 Introduction

Stimuli-responsive hydrogels are fascinating materials with potential applications in biomedicine drug delivery, separation and protein immobilization. Especially, polymer hydrogels as chemical sensors have received intensively attention in the recent decades. Takashi Miyata[1] studied the antigen-responsive hydrogel. They use the reversible binding between an antigen and an antibody as the crosslinking mechanism in a semi-interpenetrating network(semi-PIN) hydrogel. They suggest that this approach might permit drug delivery in response to a specific antigen. Also in recent years, with regard to the polymer film, a lot of work have been performed. John H. Hoitz and Sanford A. Asher[2] studied the polymerized colloidal crystal hydrogel films as intelligent chemical sensing materials. They reported the preparation of a material that changes color in response to a chemical signal by means of a change in diffraction (rather than absorption) properties. During the study of this kind of polymer hydrogels, Laser light scattering technique is a very effective method which is used to characterize the properties of the nanoparticles.

1.1.1 Laser Light Scattering

1.1.1.1 Mechanism of Laser Light Scattering

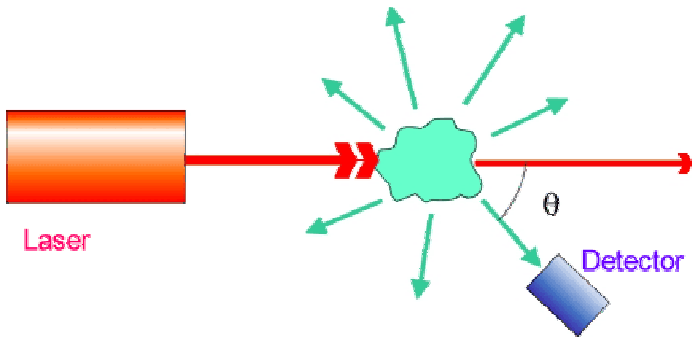

Fig.1.1 Laser Light Scattering

The interaction of the light with matter can be used to obtain important information about structure and dynamics of matter. When light is shining on matter it will scatter and the scattered light give us information about molecular structure and motion in the material.

According to the semiclassical light scattering theory[3], when light impinges on matter, the electric field of the light induces an oscillating polarization of electrons in the molecules. The molecules then serve as secondary source of light and subsequently radiate (scatter) light. The frequency shifts, the angular distribution, the polarization, and the intensity of the scatter light are determined by the size, shape and molecular interactions in the scattering material. Thus from light scattering, it should be possible, with the aid of electrodynamics and theory of time dependent statistical mechanics, to obtain information about the structure and molecular dynamics of the scattering medium.

Light scattering can be applied to both isotropic systems (e.g. liquids, polymer solution) and anisotropic systems (liquid crystals). Light scattering is capable of absolute measurements of several parameters of interest (molecular weight, radius of gyration, translational diffusion constant).

Above zero Kelvin molecules fluctuate (i.e. molecules deviate from their average position). These molecular fluctuations can be described using the molecular degrees of freedom. In the following I consider the light scattered from translational and rotational degrees of freedom which is called Rayleigh Scattering and limit ourselves to dynamic light scattering, that is, study of real-time dynamics of the system.

1.1.1.2 DLS and Polymers

Dynamic Light Scattering is a very powerful method to characterize the polymers. It can provide the information about the dynamics of a system, such as diffusion of spheres, thermal undulation of polymers and also it can give the hydrodynamic radius of the polymers. In dynamic light scattering one measures the time dependence of the light scattered from a very small region of solution, over a time range from tenths of a microsecond to milliseconds. These fluctuations in the intensity of the scattered light are related to the rate of diffusion of molecules in and out of the region being studied

(Brownian motion), and the data can be analyzed to directly give the diffusion coefficients of the particles doing the scattering. When multiple species are present, a distribution of diffusion coefficients is seen.

Traditionally, rather than presenting the data in terms of diffusion coefficients, the data are processed to give the "size" of the particles (radius or diameter). The relation between diffusion and particle size is based on theoretical relationships for the Brownian motion of spherical particles, originally derived by Einstein. The "hydrodynamic diameter" or "Stokes radius", R_h, derived from this method is the size of a spherical particle that would have a diffusion coefficient equal to that of the polymer.

Most polymers are certainly not spherical, and their apparent hydrodynamic size depends on their shape (conformation) as well as their molecular mass. Further, their diffusions are also affected by water molecules which are bound or entrapped by the polymer. Therefore, this hydrodynamic size can differ significantly from the true physical size (*e.g.* that seen by NMR or x-ray crystallography).

The strength of dynamic scattering is its ability to analyze samples containing broad distributions of species of widely differing molecular masses (*e.g.* a native protein and various sizes of aggregates), and to detect very small amounts of the higher mass species (<0.01% in many cases).

Dynamic scattering can be quite useful for assessing aggregate formation over time, and directly comparing rates of degradation for different formulations. Accelerated stability studies can be carried out by monitoring a single sample *in situ* by periodic sampling of multiple samples held at elevated temperature.

Probably the primary drawback of dynamic light scattering is that it is often difficult to accurately quantitate the amount of any aggregates that may be present. Nonetheless it can be a very good technique for relative comparisons, such as indicating which formulation, sample treatment, or purification process produces more aggregates.

1.1.2 Hydrogel

Hydrogels are three-dimensional and hydrophilic polymer networks capable of imbibing large amounts of water or biological fluids. Further more hydrogels are usually made of hydrophilic polymer molecules that are crosslinked either by chemical bonds or other cohesion forces such as ionic interaction, hydrogen bonding or hydrophobic interaction. Hydrogels are elastic solids in the sense that there exists a remembered reference configuration to which the system returns even after being deformed for a very long time.

Hydrogels have been a topic of extensive research because of their unique bulk and surface properties. Although the research on hydrogels is more than three decades old, the research interest in hydrogels is growing. Since the first report on the biomedical use of poly(2-hydroxyethylmethacrylate) hydrogel[4], hydrogels with various properties have been prepared. Hydrogels has been developed which undergo abrupt, reversible changes in volume in response to minor changes in the environment, such as solvent composition, temperature, pH, ionic strength, electric field, light intensity, pressure as well as specific chemical stimuli. Hydrogels undergoing volume transitions due to changes of the temperature have been termed 'thermally sensitive' hydrogels[5]. These types of hydrogels will suddenly shrink as the temperature increases above a critical temperature, which is approximately the lower critical solution temperature (LCST) of the corresponding linear polymer. Hydrogels can resemble natural living tissue due to their high water contents and soft touch. Hydrogels may also show a swelling behavior depending on the external environments. The most commonly studied hydrogels having environmental sensitivity are either pH[6] or temperature-sensitive[7].

In the case of thermo-sensitive hydrogels, poly(N-isopropylacrylamide) (PNIPAAm) is well-known to be the best example due to its lower critical solution temperature(LCST) behavior at around 34^0C in aqueous solution. PNIPAAm chains hydrate to form expanded structures in water when the solution temperature is below its LCST but becomes compact structure by dehydration when heated up above the LCST[8]. The PNIPAAm microgel dispersion was first synthesized in 1986[53]. Narrowly distributed microgel particles were obtained using surfactant free polymerization. Similar to the PNIPAAm macrogel, the PNIPAAm microgel particles swell in water at room temperature but shrinks and undergoes a reversible volume phase transition around 32^0C[9]. Because the diameter (less than 1um) of a microgel is much smaller than that of a macrogel (usually larger than 1mm), the microgel

responses to the environmental much faster than does the macrogel. Another thermo-sensitive gel poly(methyl vinyl ether) (PMVE), was also structurally characterized by field emission scanning electron microscopy (FESEM)[10].

For pH-sensitive hydrogels, either acid or basic pendent groups were contained in the network. Many researchers have investigated on the fast response hydrogels according to the surrounding environment. Hoffman et al. synthesized fast temperature responsive, macroporous PNIPAAm gels[11]. Okano et al. prepared a thermo-sensitive PNIPAAm hydrogels having PNIPAAm chains grafted on the backbone PNIPAAm network[12, 13]. They also reported comb-type graft hydrogels composed of poly(ethylene oxide) (PEO) graft chains in PNIPAAm network[14]. These results showed rapid gel swelling-deswelling kinetics. A fast response is necessary for applications such as artificial muscles and/or rapidly acting acutators. Alignate/PNIPAAm-NH_2 comb-type graft hydrogels which were able to respond rapidly to both temperature and pH changes were also studied[9].

1.1.3 Polymer Film Introduction

The physical and mechanical properties of thin polymer films are important from both an academic and an industrial point of view. These properties are affected not only by the nature of the polymer, but also by the method of film preparation and conditioning. Normally the preparation of the film mainly includes the following two phases:

1.1.3.1 Casting Method

There are some casting methods that serve as academic study object:

1. Casting onto photographic paper and removing the film by soaking in warm water to dissolve the gelatin.
2. Casting onto silanised plate glass and into PTFE dishes, in which case the film is removed by gently peeling it from the substrate.
3. Flash coating method that is achieved by spraying the latex onto a heated block, coated with PTFE, at temperatures exceeding 393K.
4. Casting films onto Pyrex glass plates, from which they could be removed by soaking in hot water or in the case of additive-present films, casting onto nylon plates from which the films could be removed without soaking.
5. Casting onto mercury surface.

The advantage of these methods is that the film is free of any substrate and ease of removal of the film from its casting substrate.

1.1.3.2 Film Formation

The formation of a latex film arises from the coalescence of the individual latex particles that are normally held apart by stabilizing forces (electrostatic and/or steric) resulting from the charged polymer chain end groups or surfactant. These forces are overcome by the evaporation of the continuous phase.

Minimum film formation temperature (MFFT) is a very important property during the process of forming polymer film. It depends on the elastic modulus (resistance to particle deformation), and to a lesser extent, the viscosity of the polymer. If the film is cast above its MFFT, then coalescence of the latex particles can occur. However, if the film is cast below its MFFT, then a friable discontinuous film or powder compact may form, which is typically opaque due its structured nature. The more desirable outcome of film-formation is something of a compromise since the tendency of the spheres to flow and fuse into a continuous film can, in the extreme, also result in a permanently tacky film that is more suited to adhesive applications[15].

Myers and Schultz[16] studied the formation of films at temperatures slightly lower than the MFFT by using an ultrasonic impedance technique. The results, with respect to the formation of a continuous film, were found to be dependent on the rate of drying and, hence, the rate of relief of stresses within the film. At a temperature within 6^0C below the MFFT, and with a drying rate sufficiently slow, a certain amount of creep was able to occur permitting the formation of a film due to the stresses being at a level insufficient to fracture the film. As the rate of drying was increased, the creep mechanism was not fast enough to relieve the stress such that initially the films became craxed, and at the highest drying rates, cracked.

Eckersley[17] and Jensen[18] have reported the MFFT of various polymers to be above or below the glass transition temperature (T_g) although the MFFT tends to be close to the T_g of a given polymer. They found both the MFFT and T_g are influenced by the same molecular features (e.g. The inclusion of a softer polymer will lower both the T_g and MFFT). Ellgood[19] studied a series of vinylidene chloride (VDC)/ethyl acrylate copolymers and reported both the T_g and MFFT peaked with increasing VDC content, but not at the same composition. Below 55% VDC content, the Tg was found to be greater

than the MFFT. A 15^0C difference was found between the T_g and MFFT at the extremes, and different surfactants were also found to alter the MFFT and its relationship to the T_g of the copolymer. The method of feed of a second stage monomer (e.g. seeded growth or blend) can lead to variation in the MFFT of the resultant latex due to the change in particle morphology[20]. The effect of core-shell morphology on the MFFT has, however, been found to depend on shell thickness[21] : thin soft shells on hard cores requiring higher drying temperatures than thicker soft shells due to the necessity to deform the core of the former in order to form a film.

Brodnyan and Konan[22] and Kast[23] note that comonomers that impart hydrophilic properties (eg, methyl and ethyl acrylates, etc.) into a polymer may reduce the MFFT to below the T_g, in the case of the wet film (as opposed to these properties being measured for the dry polymer) by allowing water to act as a plasticizer. Similarly, surfactant that is compatible with the polymer may also plasticize the polymer, lowering both the T_g and/or the MFFT[24, 25]. Eckersley and Rudin[17], Jensen and Morgan[18] and Sperry et al [26]. each found the MFFT to be related to latex particle size, although this is not always the case [Brodnyan and Konan[22]] (cf. the theories of film formation). Eckersley found the MFFT to be dependent on latex particle diameter and even in the case of a series of polydisperse copolymer latices, the results suggested that the MFFT be proportional to the number average particle diameter. However, the increase in MFFT between 150 nm latex and 1200 nm latex was only 5^0C. Jensen and Morgan[18] found that as the latex particle size decreased by a factor of seven, the MFFT was reduced by 10^0C. Sperry[26] found the time dependent dry MFFT (i.e. the transition from a cloudy to clear film in a latex pre-dried below its MFFT) increased with increasing particle size, and concluded that this was due to a simple viscous flow model which accounted for the larger interstitial voids which were present between larger particles and the longer time required for them to be filled (by particle deformation) to give a transparent film.

Following the evaporative drying process (typically by gravimetric methods, although Cansell et al. [27] described an alternate method using dielectric measurements), from beginning (i.e. wet latex) to end (i.e. film) leads to a sigmoidal curve, which can be divided into a number of stages for analysis. Poehlein[28] and Vanderhoff et al[29]. studied drying with and without the aid of a 'windtunnel' to remove the humidity of the evaporating water. The drying process may be complicated, however, by virtue of it being non-uniform (i.e. different areas of the film may dry at different rates) and, hence,

quantitative evaluations of the rate of drying typically involve the use of estimates of the size of, for example, dried areas of film, or the use of averages to give a mean value for the film as a whole. Despite this, attempts have been made to mathematically model the evaporative process [e.g. Pramojaney et al [30]].

Bierwagon[31] considered film formation in relation to the same three regimes as proposed by Vanderhoff, discussing drying in terms of film thickness and latex solids content. A film of low solids content could dry faster than one of high solids content despite the lower quantity of water to be removed from the latter, which however, reaches the diffusion-controlled stage (i.e. surface closure) sooner, and then loses water more slowly. As the film dries from the surface down, a fixed film area is then subject to contraction in the z-plane, thereby producing stress in the x-y plane. If polymer elasticity is insufficient, then the stress can be overcome by slippage between the coalesced layer and the fluid beneath giving rise to the 'mud-cracked' surface effect.

Hwa[32] studied the non-uniformity of film drying to determine that, as the aqueous phase evaporated, three distinct regions could be observed, e.g. a dry region, a wet(latex) region, and an intermediate region of flocculated latex(such that the film as a whole embodied all three periods of Vanderhoff's drying regime). In Hwa's circular films these regions formed concentric bands, and the films dried from the outside inwards. It was noted that these rings differed, dependent on the T_g of the polymer. In the case of a low T_g polymer, the flocculated and dry regions were both continuous, whereas for hard polymers, fine radial cracks were apparent, due to the relief of stresses, and the dry region was more opaque (due to cracks) than the flocculated region. Hwa was able to show that the particles were not close packed (the volume fraction, Φ, was between 0.49 & 0.62) such that the region was porous. The flocculation was found to be dependent, to some extent, on the nature of the surfactant used: easily desorbed soaps were proposed to be squeezed away from the points of particle-particle contact to form micelles in the particle interstices and, hence, aid flocculation, compared to the surfactant-free latex, which surfactant was not easily desorbed, however, delayed the onset of flocculation to high volume fractions.

The fact that latex of differing stability will flocculate at different particle-particle separations (i.e. at different rates) has been used to advantage by Okubo and He[33] in the preparation of asymmetric

films form latex blends. Such films showed side-dependent (i.e. polymer-substrate or polymer-air interface) variation in properties such as film tackiness and permeability.

Armstrong and Wright[34] noted that the films prepared form latex of a relatively large particle size (750nm) were of a poorer quality (i.e. poorer corrosion resistance due to greater porosity) than those films prepared from latex of a smaller particle size (105 nm). This was ascribed to the larger particles showing less coalescence, but it was not clear whether the poor quality of the film was the result of differing rates of drying resulting from the differing particles sizes, or simply due to the larger interparticle voids that would be found for the larger sized uncoalesced particles.

1.1.3.3 Theories of Film Formation

Over the years a number of theories regarding the formation of polymer films, form the fusion of latex particle spheres, have been considered. These include:

1. Dry sintering[35, 36]
2. Wet sintering[37]
3. Piston-like compression[38] arising from the preferentially dried surface layer building in thickness form the top down;
4. Interparticle cohesion promoted by surface forces[39].

Dry sintering is driven by the polymer-air surface tension. Dillon et al. [35] discuss the coalescence processes in terms of the viscous flow of the polymer. This viscous flow was result from the shearing stress caused by the decreasing in the polymer-particle surface area, and the resultant decrease in polymer surface energy as the film is formed.

Brown[37] discussed **wet sintering**, driven by the polymer-water interfacial tension, leading to the deformation of particles, during drying. He considered the forces acting both for and against the coalescence of the latex particles, with the conclusion that for coalescence to occur, and inequality must exist in which the capillary force, F_C, (resulting form the surface tension of the interstitial water, caused by the formation of small radii of curvature between the particles as the water evaporated) must overcome the forces of resistance to deformation, F_G, of the latex spheres: i.e. $F_C > F_G$. These forces, Brown presumed, were proportional to the relevant pressures, with the area over which they act as the constant of proportionality, and hence: $P_C > P_G$. From Laplace's equation, Brown derived the capillary

pressure, P_C for the cylinder of radius R, between three contiguous latex particles, in terms of the latex particle radii, r:

$$P_C = (2\gamma_w / R) = 12.9\ \gamma_w / r$$

Where γ_w is the polymer-water interfacial surface tension;

Note:

$$R / (R + r) = \cos 30^0$$

By treating the particles as elastic bodies, the pressure on the area of contact was also calculated, in terms of the elastic shear modulus, G, of the polymer and, hence, Brown derived an expression for coalescence:

$$G_t < 35\ \gamma_w / r$$

Where G_t is time dependent shear modulus (necessary because the viscoelastic particles are treated as elastic); r = latex particle radius.

Sheetz[38] also formulated his own theory of latex coalescence. In qualitative terms, as the latex becomes concentrated by evaporation of the water, flocculation occurs as the repulsive forces of the particles are overcome. Particles at the latex-air interface are then subject to the forces for capillarity and therefore coalescence, leading to compaction and deformation of the particles under the surface. Water in the film's interior must then diffuse through the upper layers to escape and this generates further, vacuum-like, compressive force acting normal to the film's surface. The mechanism therefore seem to be based on Brown's wet sintering mechanism and diffusion. Scheetz analyzed the thermodynamics of the system and showed that the source of the energy for the particles' fusion was the heat in the environment-converted for film formation by the evaporation of the water. In evidence for the diffusion being involved in the coalescence mechanism, Sheetz cited the facts that a film containing a water-permeable polymer dried at a rate faster than one that was less water permeable; and that a film in which capillary action was prevented (by means of a thin solvent-cast film) could form a continuous film, whilst the same polymer without the solvent-cast deposit formed a discontinuous film.

Although Dobler et al.[40] generally agreed with the mechanism of Scheetz, they believed, from observations of iridescence, that the surface of the latex closes (i.e. complete surface iridescence followed, presumably, by skin formation) long before the particles become close packed in the bulk latex (as they do in Sheetz's theory).

Like Sheetz, Mason[41] also identified a number of erroneous assumptions and points of error in Brown's work. Mason points out that these areas (over which F_C and F_G act) are not necessarily identical, and repeated the analysis using corrected values for the areas such that the condition Brown quoted became:

$$G < 67.6\gamma_w / r$$

Mason also criticizes the fact that Brown assumed that the capillary pressure remained constant whilst the latex particles coalesced, and derived a new equation for the capillary pressure based on the deformation of the spheres. From this, the criterion for film formation moved yet further from Brown's inequality, to give:

$$G < 266\gamma_w / r$$

It also has been noticed[42] that Brown's work has been criticized for using a polymer modulus which was obtained for the dried polymer, rather than a polymer in an aqueous environment.

Despite Brown's differences with Dillon over the role of the evaporating water phase in latex coalescence mechanisms, both research groups presumed that the forces of coalescence were inversely proportional to the latex particle radii. Vanderhoff et al. [43, 44, 45] indicated that the pressures for coalescence, resulting from the works of Dillon and Brown, were insufficient to cause the coalescence of particles greater than 1um in diameter and extended the theories accordingly. These extensions to the theory were again based on determining the forces acting to cause coalescence.

1.1.3.4 Solvent-Casting of Film

Whilst the formation of films from latex and from polymers in solution may seem to be fundamentally different processes, there are aspects of similarity: e.g. macromolecules in solution behave hydrodynamically as though they are molecular dispersions having solvent-impermeable cores and peripheral solvent-permeable segments[46]; a difference mainly of scale compared with uncharged sterically stabilized latex particles. Whether solvents will necessarily deposit pore-free films of the maximum density and lowest permeability is uncertain. Different outcomes are predicted[47-49], depending upon the solvent power, when high concentrations are reached in the later stages of drying.

The rate of evaporation of solvent from solvent-cast films depends upon the square root of the time as expected for a process controlled, or limited, by diffusion, i.e. Fickian desorption to the surface through a homogeneous solution of increasing the concentration[50]. However, the removal of the final traces of solvent form solvent-cast films is a problem: attributed to the fact that the polymer may be plasticized by the solvent. Elevated temperature (to assist diffusion of the solvent in the polymer), good vacuum and long drying times are used to overcome the problems[51]. The removal of the final traces of solvent can be important with regard to toxicity (in the case of pharmaceutical coatings) and also the permeability properties of solvent-cast coatings. List and Laun[52] found the water vapor permeability of isopropyl alcohol-cast films to be markedly increased by residual solvent. However, effects of the residual solvent were minimized by secondary drying, and the solvent could be almost completely removed in a very short time (8 hrs) if the film was held above its T_g.

1.1.4. Studies on PNIPAAm Hydrogel

As discussed before, due to the unique thermo-sensitive property of PNIPAAm whose phase transition temperature is around 34^0C, a lot of studies about PNIPAAm have been performed in this field since the first PNIPAAm microgel was made in 1986[53]. The volume phase transition of the PNIPAAm microgel has been studied and compared with bulk gel and linear polymers using light scattering technique[54]. Rheological properties of the PNIPAAm colloidal dispersion have also been investigated[55]. The viscosity of the PNIPAAm microgel dispersion can be changed by two orders of magnitude by the temperature-induced swelling of the particles. The neutral and monodispersed PNIPAAm microgel particles can form colloidal crystals and glasses in concentrated dispersions[61]. This behavior is similar to that of hard spheres[56]. On the other hand, ionized PNIPAAm colloidal dispersion can be electrostatically stabilized and form a colloidal crystal at a lower polymer content[57]. Such an array may have potential for sensor applications. The research progress in PNIPAAm polymer solution, macrogel, and microgel dispersions can be found in several excellent reviews[58, 59, 60]. There are also a lot of studies mainly concentrating on the study of the behavior of PNIPAAm during phase-transition[61] , the behavior of the charged (positive or negative) PNIPAAm gel[62], the interaction between PNIPAAm and surfactant[63] and also the size control of PNIPAAm particle[64]. However, the study of PNIPAAm as polymer film has not been widely studied, its unique shape-memory effect has potential in practical applications. In our experiments, the thermo-sensitive colored PNIPAAm was

prepared, the shape-memory effect was observed and the turbidity method was performed to investigate the film formation.

1.2 Experimental

N-isopropylacrylamide(NIPAAm, Polysciences Inc.), N, N' -methylene-bis-acrylamide (BIS, Bio-Rad laboratories), acrylic acid (AA, 99%, Aldrich Chemical Company, Inc.), dodecyl sulfate, sodium salt (SDS, 98%, Aldrich Chemical Company, Inc.), potassium persulfate (KPS, 99%, Aldrich Chemical Company, Inc.) and epichlorohydrin (EPO, 99%, Aldrich Chemical Company, Inc.) were used as received.

Our light scattering hardware setup consists of a commercial equipment for simultaneous static and dynamic experiments by ALV-5000 (Langen, Germany). I use the red light (632.5 nm) of a He-Ne ion laser at a power output of 0.1-200 mW. The primary beam's intensity and position were monitored by means of a beam splitter and a four-segment photodiode. The thermostated sample cell is placed on a motor-driven precision geonometer (±0,001 which enables the photomultiplier detector to be moved accurately from 20 to 150scattering angle.)

PNIPAAm Hydrogel Preparation

The experiments were conducted in a 500 ml glass polymerization reactor with a nitrogen bubbling tube and a PTFE stirrer. The reactor was immersed into a water bath set at 70^0C. 3.80g NIPA, 0.0665g BIS, 0.11g AA, some amount of SDS (in my experiment I prepared the hydrogels with different nanoparticle size by adjusting the amount of the surfactant SDS. The latex recipe is listed in Table I) was added into the reactor, diluted with deionized water to 250ml solution. The solution was stirred at 300 rpm for 30min with a nitrogen purge to remove the oxygen inside the solution. KPS (16.6g (1%) solution) was added and the reaction was stirred for 4 hours under 70^0C.

The reaction was carried out until the reactor cooled down to the room temperature. The solution was put into a vial (23 × 85mm) and precipitated with acetone at the most extent. The top clear solution was discarded and the precipitate was collected. The above steps were repeated three to five times, all of the precipitate were collected and dried with a dryer for two days in order to discard the water as complete as possible. Furthermore, after the drying process, The precipitated was dissolved with acetone and was vaporized for removing the rest water inside the precipitate completely. The latex particles were mixed with epichlorohydrin (cross-linking agent) to a homogeneous state using

Fisher Vortex Genie 2^{TM}. The gelation was completed by putting the vial into the oven under temperature 80^0C-90^0C for 6hrs.

Film Preparation

A small amount of latex made in the above steps was put into a vial. After the vial was sealed, it was put into the oven under 70^0C for 3 hrs. Water was then added into the vial at room temperature, the film obtained was put into a big beaker.

DLS Experiment

The nanoparticle size before cross-linking was measured by dynamic light scattering method and data analysis was done with ALV software. In this experiment, a commercial LLS spectrometer (ALV/DLS/SLS-5000) equipped with an ALV-5000 digital time correlator was used with a Helium-Neon laser (Uniphase 1145P, output power of 22 mw and wavelength of 632.8 nm) as the light source. The incident light was vertically polarized with respect to the scattering plane and the light intensity was regulated with a beam attenuator (Newport M-925B). The scattered light was conducted through a thin (~ 40 um in diameter) optic fiber leading to an active quenched avalanche photo diode (APD), the detector.

Turbidity Experiment

The turbidity of the film was measured by using UV-VIS spectrophotometer. The UV-visible absorbance spectra were measured at 1 nm resolution on a diode array spectrometer (Hewlett-Parkard, Model 8543) with the wavelength range from 190 to 1100 nm. Quartz cells with inner dimensions of 10 mm x 10 mm x 42 mm (Fisher Sceintific QS1.000) were used. The turbidity of the sample was obtained from the ratio of the transmitted light intensity to the incident intensity as $\alpha = -(1/L)\ln(I_t/I_0)$, where L was the sample thickness (10 mm). The temperature of samples was controlled by a circulation water bath (Brinkmam Lauda Super RM-6) with control accuracy of $\pm$ 0.02 ^{0}C.

TABLE 1

Chemicals	I	II	III	IV	V	VI	VII
NIPA(g)	3.80	3.80	3.80	3.80	3.80	3.80	3.80
BIS(g)	0.066	0.066	0.066	0.066	0.066	0.066	0.066
SDS(g)	0.21	0.17	0.12	0.08	0.06	0.04	0
AA(g)	0.11	0.11	0.11	0.11	0.11	0.11	0.11
KPS(1%, g)	16.6	16.6	16.6	16.6	16.6	16.6	16.6

1.3 RESULTS and DISCUSSION

1.3.1 Reaction Mechanism

The reaction mechanism was proposed in Fig.1.2. During the first phase, the PNIPAAm nanoparticle were synthesized by free-radical polymerization. After that, epichlorohydrin was used as crosslinker to form the PNIPAAm hydrogel. In my experiment, the PNIPAAm film was casted onto glass. The cross-linking included two steps. First, NIPAAm monomer and BIS and Acrylic Acid (AA) under 70^0C reacted by free-radical polymerization initiated by potassium persulfate (KPS) and formed nanoparticle with hydroxyl functional group latex. Second, epichlorohydrin (EPO)was used as a crosslinker to form the hydrogel network.

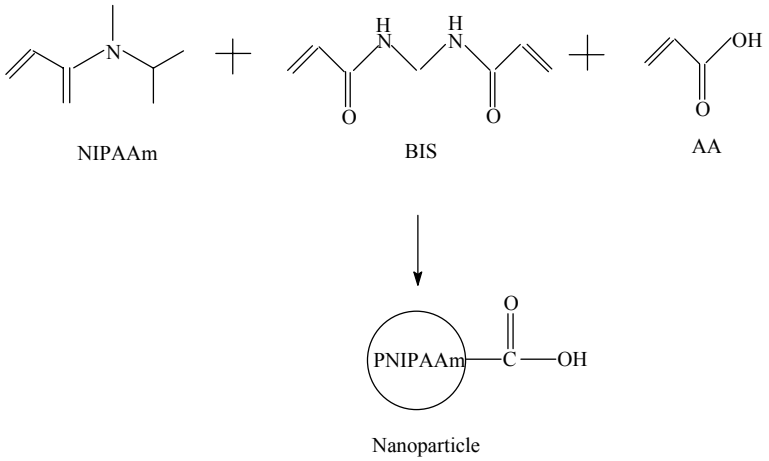

(a)

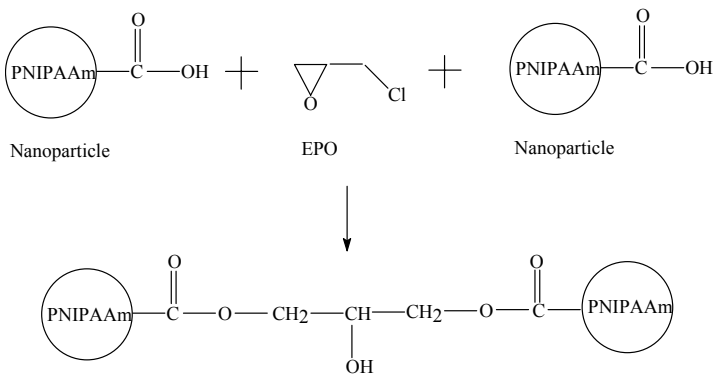

(b)

Fig.1.2 Reaction Mechanism (a) PNIPAAm latex formation (b) PNIPAAm hydrogel network formation

1.3.2 Image of PNIPAAm Hydrogel Film

The pictures of the film were taken at different angles, shown in Fig. 1.3. From these two pictures I found there are some differences with regard to the color of the film. For the lateral picture, the film is blue-green color. But if seeing it from top, it is blue. That is because of the refraction caused by the different refraction index between water and hydrogel network and the ordering packed nanoparticles in the film.

(a)

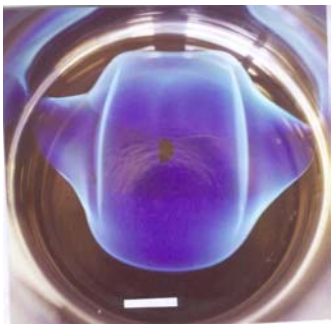

(b)

Fig.1.3 The pictures of film taken under different angles (a) Side view (b) Top view

1.3.3 The Shape-Memory Effect

When the temperature was increased from 25^0C to 42^0C, the color of the film was changed into white-opaque from the original blue-green. This is understandable because when the temperature is increased, the water inside the hydrogel has been expelled to the outside which leads to the inflecting index of the nanoparticle decreasing, so the transparency of the film decreased. And also the figure of the original film has changed which is shown in Fig. 1.4. The most interesting thing is that when decreasing the temperature from 42^0C back to the room temperature, the film can recover its original figure without any change. The reason I thought is due to the decreasing of the temperature which will lead the water to be absorbed into the hydrogel network again. Fig.1.4 shows the shape-memory effect.

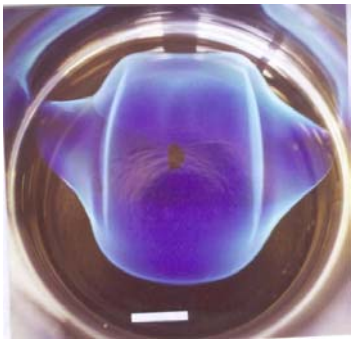

increase T ↓↑decrease T

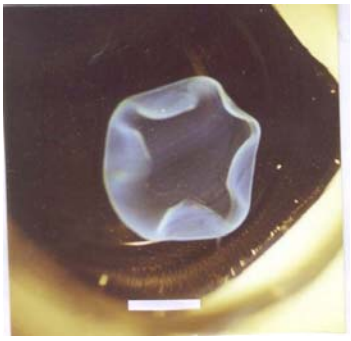

Fig.1.4 Shape-memory effect

1.3.4 DLS measurement of PNIPAAm Nanoparticle

The dynamic light scattering method was used to measured the hydrodynamic radius of the PNIPAAm nanoparticles before further crosslinking. Very sharp peaks were obtained. These peaks show very narrow molecular weight distribution, which shows that the latex is almost in a mono-dispersed state. The experiment results are shown in Fig. 1.5.

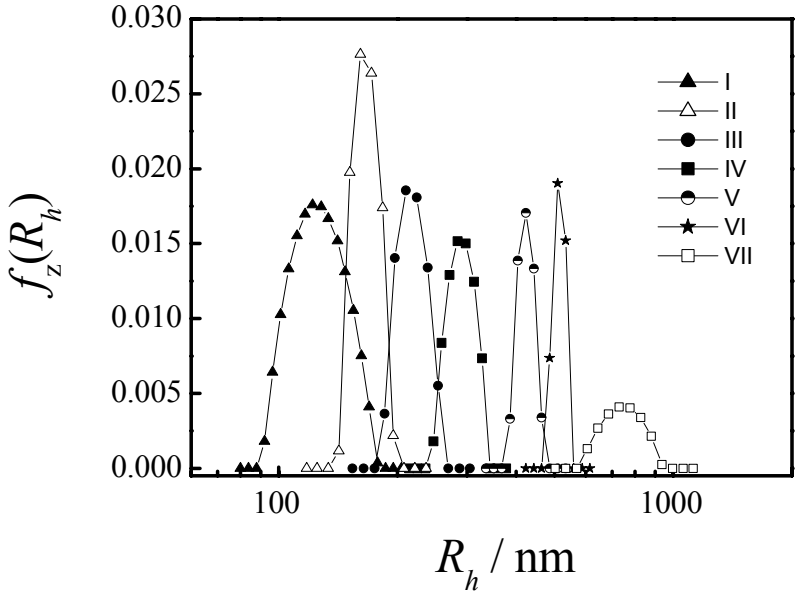

Fig. 1.5 PNIPAAm particle size distribution (solvent: water), the SDS amount are : I (0.21g), II (0.17g), III (0.12g), IV (0.08g), V(0.06g), VI(0.04g), VII (0.0g)

From Fig. 1.5, we can conclude that the PNIPAAm particle size can be easily controlled by adjusting the amount of surfactant added, which is very important to our future study.

1.3.5 The Turbidity Experiment

In order to reveal the behavior of PNIPAAm film, the temperature-dependent of turbidity of PNIPAAm thin film was measured using a HP UV-Visible spectrophotometer as shown in Fig.1.6. In the first region from 29^0C to 40^0C, when the temperature increases, the water lies between the PNIPAAm nanoparticles was expelled outside the whole network, which results the whole network from a homogeneous state to a heterogeneous state leading to the decreasing of transmittance of the film. In the second region from 40^0C~46^0C, all the water between the nanoparticles was expelled from the network making the network to a homogeneous state again. As a result, the absorbance of the film decreases. In the third region above 46^0C, when the temperature increases, the homogeneous state was destroyed again by expelling the water inside the nanoparticles out of network so that the network

becomes a heterogeneous state again, therefore the absorbance of the film increased again resulting the opaqueness of the film. This effect is reversible as the temperature was cycles between 29^0C and 56^0C.

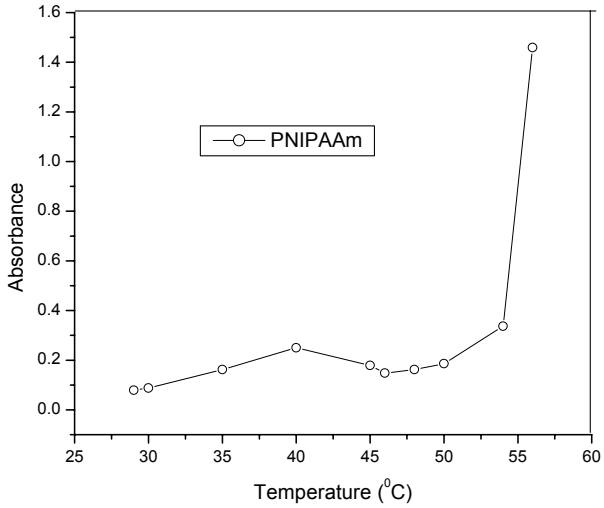

Fig. 1.6 Temperature-dependent of turbidity of PNIPAAm film

1.3.6 Conclusion

Thermo-sensitive colored PNIPAAm hydrogel films were synthesized by firstly synthesizing latex and secondarily crosslinking. Their properties changes in response to environmental temperature changes. Such intelligent hydrogels might be used in chemomechanical systems and separation devices as well as sensors, further study is still in progress.

CHAPTER 1 REFERENCE:

[1] Takashi Miyata, Noriko Asami, Tadashi Uragami, “A reversibly antigen-responsive hydrogel” , Nature 399, 766-769(1999)

[2] Intelligent Polymerized Crystalline Colloidal Arrays: Novel Chemical Sensor Materials, J. H. Holtz, J. S. W. Holtz, C. H. Munro, and S. A. Asher, *Anal. Chem*. **70**, 780 (1998).

[3] Berne and Pecora, "Dynamic Light scattering" John Wiley, 1975

[4] Wichterle, O. and D. Lim. “Hydrophilic Gels for Biological Use”. Nature, 185: 117-118, 1960

[5] Hoffman, A. S. 1987. “Application of Thermally Reversible polymers and Hydrogels in Therapeutics and Diagnostics”, J. Controlled Rel. , 6:297-305

[6] N.A. Peppas, P. Bures, W. Leobandung and H. Ichikawa. Eur J Pharm Biopharm 50, pp.27-46, 2000.

[7] O. Hirasa, S. Ito, A. Yamauchi, S. Fujishige and H. Ichijo. In: Polymer gels, fundmentals and biomedical application, Plenum Press, New York, pp. 247-256, 1991.

[8] Kim SY, Cho SM, Lee YM. J Appl Polym Sci, 78:1381- 91, 2000.

[9] Hee Kyung Ju, So Yeon Kim, Young Moo Lee Polymer Vol. 42, Issue 16, 6851-6857, 2001

[10] Karl-Fr Arndt, Thomas Schmidt and Rudolf Reichelt Polymer, Volume 42, Issue 16, 6785-6791, 2001

[11] X.S. Wu, A.S. Hoffm, 2001an and P. Yager. J Polym Sci, Part A: Polym Chem 30, pp. 2121-2129, 1992

[12] R. Yoshida, K. Uchida, Y. Kaneko, K. Sakai, A. Kikuchi, Y. Sakurai and T. Okano. Nature 374 16, 240-242, 1995.

[13] Y. Kaneko, K. Sakai, A. Kikuchi, R. Yoshida, Y. Sakurai and T. Okano. Macromolecules 28, 7717-7723, 1995.

[14] Y. Kaneko, S. Nakamura, K. Sakai, T. Aoyagi, A. Kikuchi, Y. Sakurai and T. Okano. Macromolecules 31, 6099-6105, 1998.

[15] Talen H.W., Hover P.F., Deutsche Farben Z, 13, 50-55, 1959. (CBDE Translation.)

[16] Myers R.R., Schultz R.K., J. Appl. Polym. Sci., 8, 755-764, 1964.

[17] Eckersley S.T., Rudin A., J. Coatings Technol., 62 (780), 89-100, 1990.

[18] Jensen D.P., Morgan L.W., J. Appl. Polymer Sci., 42, 2845-2849, 1991.

[19] Ellgood B., J. Oil & Colour Chem. Assoc., 68, 164-169, 1985.

[20] Cao T., Xu Y., Wang Y., Chen X., Zheng A., Polym. Int., 32, 153-158, 1993.

[21] Devon M.J., Gardon J.L., Roberts G., Rudin A., J. Appl. Polym. Sci., 39, 2119-2128, 1990.

[22] Brodnyan J.G., Konen T., J. Appl. Polym. Sci., 8, 687-697, 1964.

[23] Kast H., Makromol. Chem., Suppl. 10/11, 447-461, 1985.

[24] Eckersley S.T., Rudin A., J. Appl. Polym. Sci., 48, 1369-1381, 1993.

[25] Vijayendran B.R., Bone T., Gajria C., In Some Studies on Vinyl Acrylic Latex- Surfactant Interactions., Emulsion Polym. Vinyl Acetate Pap. Symp. J., Meeting 1980 Ed., 253-283, (1980).

[26] Sperry P.R., Snyder B.S., O'Dowd M.L.m Lesko P.M., Langmuir, 10, 2619-2628, 1994.

[27] Cansell F., Henry F., Pichot C., J. Appl. Polym. Sci., 41, 547-563, 1990.

[28] Poehlein G.W., Vanderhoff J.W., Witmeyer R., J. Polym. Preprints, 16 (1), 268-273, 1975.

[29] Vanderhoff J.W., Bradford E.B., Carrington W.K., J. Polym. Sci., Polym. Symp. 41, 155-174, 1973.

[30] Pramojaney N., Poehlein G.W., Vanderhoff J.W., Drying '80, 2, 93-100, 1980.

[31] Bierwagon G.P., J. Coatings Technol., 51 (658), 117-129, 1979.

[32] Hwa J.C.H., J. Polym. Sci., A (2), 785-796, 1964.

[33] Okubo M., He Y., J. Appl. Polym. Sci., 42 (8), 2205-2208, 1991.

[34] Armstrong R.D., Wright J.D., Corrosion Sci., 33 (10), 1529-1539, 1992.

[35] Dillon R.E., Matheson L.A., Bradford E.B., J. Colloid Sci., 6, 108-117, 1951.

[36] Frenkal J., J. Phys. (USSR), 9, 385, 1943.

[37] Brown G.L., J. Polym. Sci., 22, 423-434, 1956.

[38] Sheetz D.P., J. Appl. Polym. Sci., 9, 3759-3773, 1965.

[39] Kendall K., Padget J.C., Int. J. Adhesion and Adhesives, 2, 149-154, 1982.

[40] Dobler F., Pith T., Lambla M., Holl Y., J. Colloid and Interface Sci., 152, 1, 1992.

[41] Mason G., Brit. Polym. J., 5, 101-108, 1973.

[42] Kan C.S., Advaced Coating Fundamentals, TAPPI Notes, 101-107, 1993.

[43] Vanderhoff J.W., Tarkowski H.L., Jenkins M.C., Bradford E.B., J. Macromol. Chem., 1 (2), 361-397, 1966.

[44] Vanderhoff J.W., Br. Polym. J., 2, 161-172, 1970.

[45] Vanderhoff J.W., Paint and Varnish Prod., 25-37, Dec. 1970.

[46] Napper D.H., Gilbert R.G., Emulsion Polymerization: The Mechanisms of Latex Particle Formation and Growth., in An Introduction to Polymer Colloids., Eds F. Candau, R.H. Ottewill, Pub. KluIr Academic Publishers, 159-185, 1990.

[47] Funke W., Zorll U., Defazet, 29 (4), 146-153, 1975. (CBDE Translation.)

[48] Nicholson J.W., Wasson E.A., Film Spreading and Film Formation by Waterborne Coatings., in Surface Coatings, Ch. 2, Vol. 3, 91-123, 1990.

[49] Gould R.F., In Contact Angle, Ittability and Adhesion, Advances in Chemistry., Series 43, A.C.S., 1964.

[50] Blandin H.P., David J.C., Vergnaud J.M., Illien J.P., Malizewicz M., J. Coatings Tech., 59 (746), 27-32, 1987.

[51] Vezin W.R.,Florence A.T., European Polym. J., 17, 93-99, 1981.

[52] List P.H., Laun G., Pharm. Ind., 42 (4), 399-401, 1980.

[53] Pelton, R.H.; Chibante, P. Colloids Surf. 120, 247, 1986

[54] Wu, C. Polymer 39, 4609, 1998.

[55] Senff, H.; Richtering, W. J. Chem. Phys. 111, 1705, 1999.

[56] Pusey, P. N.; Van Megen, B. Nature 1986, 320, 340.; Meeker, S. P.; Poon, C. K.; Pusey, P. N. Phys. Rev. E. 55, 5718, 1997.

[57] Iissman, J. M; Sunkara, H. B.; Tse, A. S.; Asher, S. A. Science 274, 959, 1996.

[58] Schild, H. G. Prog. Polym. Sci. 17, 163, 1992.

[59] Shibayama, M.; Tanaka, T. Advances in Polym. Sci. 109, 1, 1993.

[60] Pelton, R. Adv. Colloid and Interf. Sci. 85, 1, 2000.

[61] R. Appel, T.W. Zerda, C. Wang, Z. Hu polymer 42, 1561-1566, 2001

[62] M. Mielke, R. Zimehl Progr Colloid Polym Sci. 111: 74-77, 1998.

[63] Wayne McPhee, Kam Chiu Tam, Robert Pelton Journal of Colloid and Interface Science 156, 24-30 (1993)

[64] R. H. Pelton, H. M. Pelton, A. Morphesis, R. L. RoIll Langmuir, 5, 816-818, 1989.

CHAPTER 2

SYNTHESIS AND CHARACTERIZATION OF SURFACTANT-FREE THREE DIMENSIONAL POLYSTYRENE NANOPARTICLE NETWORK

2.1 INTRODUCTION

Polymer adsorption plays an important role in many products and processes where stabilization or flocculation of colloidal dispersions is required. For example, polymers act as stabilizers in paints, pharmaceutical and cosmetic ointments and creams, lubricants used in the oil industry and in the production of magnetic tapes, etc. The flocculating capability of polymers is important in applications such as paper-making and waste water treatment. In all these applications, the structural stability of the polymer layer on the solid (or liquid) surface plays an important role in the usefulness of the polymers.

Among those adsorbed polymers, polystyrene (PS) is undoubtly one of the most extensively being studied polymers because of its special structure (side benzyl ring and active double bond). The preparation and application of the uniform polystyrene (PS) nanospheres is of a long history. In 1947, an electron microscopist at the university of Michigan first discovered that the polystyrene latex particles were perfect spheres[1] . Since then, these uniform particles of different sizes have been used for the calibration of various instruments., for checking openings in filters, pores and blood vessels, for packing in various chromatographic columns, for testing electrophoresis method used for protein separation (the experiment of which has been carried out in NASA's Apollo 16 mission), for latex agglutination test as indicators in certain diseases like meningitis and conditions like pregnancy, for phagocytosis research, and so on. These uniform latex particles are so useful that they have even been produced in space, on shuttle flights in early 1980's. Apart form the extensive uses of the PS latex particles as standard models for studying the interactions[2] and the adsorption of the colloidal systems, [3] and for the application of latex immunoassays[4] and drug carriers[5] , the concentrated PS latex dispersions are also used to cast films[6] and to create colloidal crystal arrays which are embedded into gel matrices either as optical sensors or as precursors of the porous arrays.

Porous cross-linked styrene-based polymers have also gained widespread use as supports for polymer bound reagents and catalysts. Presently the large majority of these materials are mainly made

by chemical modification of preformed high surface area polymers. Polymerization of a functional monomer solution, the tailored monomer approach, to yield a functional porous copolymer are also a straightforward method to avoid many drawbacks associated with multi-step chemical modification processes. The main drawback of the materials functionalized ab initio by copolymerization is the fact that, depending on the relative reactivity ratios, a part of the functional groups are buried inside inaccessible cores of cross-linked modules. The inaccessible part may become very large when formulations with enough cross-linking monomer to yield a macroporous structure are used. The location of functional species on insoluble polymer surfaces to give highly accessible regions of the cross-linked matrix is therefore of major importance in the synthesis of a porous polymer through a tailored monomer approach. The synthesis of a high surface area polymer with bis(phosphonic acid) groups located on the surface has been achieved by Jan H. Nasman[7]. This process is achieved by adding the surfactant (bis(2-ethylhexyl) sulfosuccinate sodium salt) (AOT, Fluka), it played an important role during the whole porous forming process. In addition, poly[(chloromethyl)styrene-co-divinylbenzene] as porous rods[8] and porous plug formed by mono-disperse polystyrene microspheres have also been studied [9].

With regard to the adsorption/desorption of porous polystyrene, BET (Brunauer-Emmett-Teller) which is termed the " continuous elution method" as an analytical method has been developed. In this method, preadsorbed powders are packed into a small column, solvent elution is performed and the concentration of polymer desorbed from the adsorbent surface is measured. This method can provides new information about the polymer adsorption layer and the polymer layer whose radius of gyration in the solution is roughly equal to the pore size of the adsorbent.

2.2 Theory of Adsorption[10-12]

Molecules and atoms can attach themselves onto surfaces in two ways. In physisorption (physical adsorption), there is a weak van der Waals attraction of the adsorbate to the surface. The attraction to the surface is weak but long ranged and the energy released upon accommodation to the surface is of the same order of magnitude as an enthalpy of condensation (on the order of 20 kJ/mol). During the process of physisorption, the chemical identity of the adsorbate remains intact, i.e. no breakage of the covalent structure of the adsorbate takes place. Physisorption, to be a spontaneous thermodynamic process, must have a negative free energy ΔG. Because translational degrees of

freedom of the gas phase adsorbate are lost upon deposition onto the substrate, the change of entropy ΔS is negative for this process. Since $\Delta G = \Delta H - T\Delta S$, enthalpy ΔH for physisorption must be exothermic.

In **chemisorption** (chemical adsorption), the adsorbate sticks to the solid by the formation of a chemical bond with the surface. This interaction is much stronger than physisorption, and, in general, chemisorption has more stringent requirements for the compatibility of adsorbate and surface site than physisorption. The chemisorption may be stronger than the bonds internal to the free adsorbate which can result in the dissociation of the adsorbate upon adsorption (dissociative adsorption). In some cases ΔS for dissociative adsorption can be greater than zero, which means endothermic chemisorption, although uncommon, is possible.

The energy of adsorption depends on the extent to which the available surface is covered with adsorbate molecules. This is because the adsorbates can interact with each other when they lie upon the surface (in general they would be expected to repel each other). The fractional coverage of a surface is defined by the quantity θ:

$$\theta = \frac{\text{Number of occupied adsorption sites}}{\text{Total number of possible sites}}$$

At any temperature, the adsorbate and the surface come to a dynamic equilibrium, that is, the chemical potentials of the free adsorbate and the surface bound adsorbate are equal. The chemical potential of the free adsorbate depends on the pressure of the gas p, and the chemical potential of the bound adsorbate depends on the coverage θ. Thus the coverage at a given temperature is a function of the applied adsorbate pressure. The variation of θ with p at a given T is called an adsorption isotherm.

Several adsorption isotherms have proven useful in understanding the process of adsorption. The simplest isotherm is attributed to a pioneer in the study of surface processes, Langmuir, and is called the Langmuir isotherm. If one assumes:

- Adsorption cannot proceed beyond the point at which the adsorbates are one layer thick' on the surface (monolayer)
- All adsorption sites are equivalent.
- The adsorption and desorption rate is independent of the population of neighboring sites.

then one can derive a simple formula for an adsorption isotherm[13-15]. Consider the equilibrium

$$A + S \rightleftharpoons A{\cdot}S$$

where A is the free adsorbate, S is the free surface, and A·S is the substrate bound to the surface. The rate of adsorption will be proportional to the pressure of the gas and the number of vacant sites for adsorption. If the total number of sites on the surface is N, then the rate of change of the surface coverage due to adsorption is:

$$\frac{d\theta}{dt} = k_a p N(1 - \theta)$$

The rate of change of the coverage due to the adsorbate leaving the surface (desorption) is proportional to the number of adsorbed species:

$$\frac{d\theta}{dt} = - k_d N \theta$$

In these equations, k_a and k_d are the rate constants for adsorption and desorption respectively and p is the pressure of the adsorbate gas. At equilibrium, the coverage is independent of time and thus the adsorption and desorption rates are equal. The solution to this condition gives us a relation for θ:

$$\theta = \frac{Kp}{1 + Kp}$$

where $K = k_a / k_d$. Note that because K is an equilibrium constant, the value of K at various temperatures determined from the Langmuir isotherm allows for the evaluation of the enthalpy of adsorption, ΔH_{ads}, through the van't Hoff equation:

$$\left(\frac{\partial \ln K}{\partial T} \right) = \frac{\Delta H_{ads}}{RT^2}$$

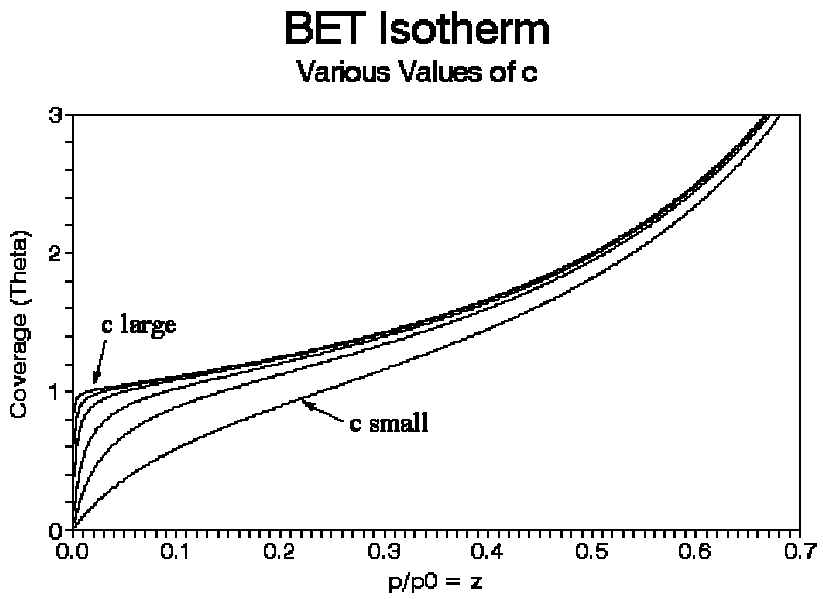

The Langmuir isotherm gives us a wonderfully simple picture of adsorption at low coverage and is applicable in some situations. At high adsorbate pressures and thus high coverage, this simple isotherm fails to predict experimental results and thus cannot provide a correct explanation of adsorption in these conditions. What is missing in the Langmuir treatment is the possibility of the initial overlayer of adsorbate acting as a substrate surface itself, allowing for more adsorption beyond a saturated (monolayer) coverage. This possibility has been treated by Brunauer, Emmett, and Teller[16] and the result is named the BET isotherm. This isotherm is useful in cases where multilayer adsorption must be considered. The form of this isotherm is:

$$\frac{n}{n_{mono}} = \frac{cz}{(1-z)\,[1-z(1-c)]} = (\theta)$$

where n/n_{mono} is the ratio of the moles adsorbed to the moles adsorbed in a single monolayer, and $z = p/p_0$, where p_0 is the vapor pressure of the pure condensed adsorbate. The n/n_{mono} ratio represents a generalized coverage because its value can exceed unity. The constant c represents the relative strengths of adsorption to the surface and condensation of the pure adsorbate. Simple theory predicts an approximate value of this constant as:

$$c \approx \frac{e^{-\Delta H_{ads}/RT}}{e^{\Delta H_{vap}/RT}}$$

The BET isotherm predicts that the amount of adsorption increases indefinitely as the pressure is increased since there is no limit to the amount of condensation of the adsorbate. In the limit that adsorption to the surface is much 'stronger' than the condensation to a liquid (such as for the adsorption of unreactive gases onto polar substrates) the BET isotherm simplifies to the form (c=∞):

$$(\theta) = \frac{1}{1-(p/p^0)} = \frac{1}{1-z}$$

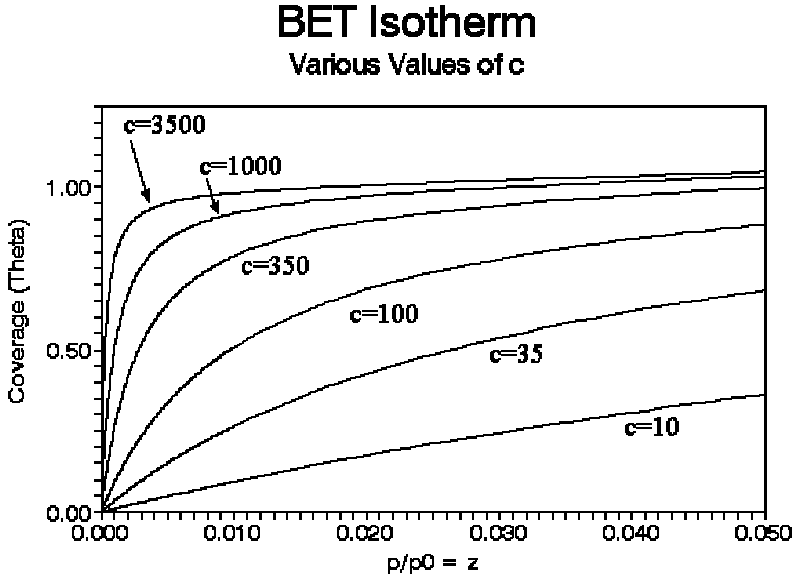

The Langmuir isotherm is found to be useful only at very small coverages (sub-monolayer) but is generally applied to all cases involving chemisorption. This would correspond to the limiting case of c approaching infinity in the BET formalism, and no insight is provided by BET below one monolayer in this limit.

The BET isotherm is found to describe adequately the physisorption at intermediate coverage (θ = 0.8 - 2.0) but fails to represent observations at low or high coverage. The BET isotherm is reasonably valid around θ=1.0, however, and this is useful in characterizing the area of the absorbent. If one can determine experimentally the number of moles of adsorbate required to give θ= 1.0 (i.e. a monolayer), one can determine the specific area of the absorbent:

$$\overline{A} = \frac{\text{surface area of absorbent } [\ m^2]}{\text{mass of absorbent } [\ g\ ]}$$

Practically, one measures the number of moles adsorbed as a function of equilibrium pressure, i.e. one does not directly measure θ. Algebraic rearrangement of the BET isotherm to produce a linear equation is usually applied to experimental data.

$$\frac{z}{n(1-z)} = \frac{1}{n_{mono}c} + \left(\frac{(c-1)}{n_{mono}c}\right) z$$

This implies that over the range where the BET isotherm is valid a plot of z / n(1-z) vs. z will be linear. The slope and intercept of this line will allow the determination of n_{mono} and c. The specific area of the sample is simply:

$$\overline{A} = N_A n_{mono} \sigma / m$$

The adsorption process is generally taken as completely reversible, but, under some conditions the isotherm may exhibit a different shape upon desorption as compared to absorption. This is called **hysteresis**. Sometimes hysteresis data can be used to determine the structure and size of pores in the absorbent. We will therefore need to generate an isotherm for both absorption and desorption. The following is one kind of adsorption measurement equipment called Omnisorb360 which is a commercial vacuum manifold :

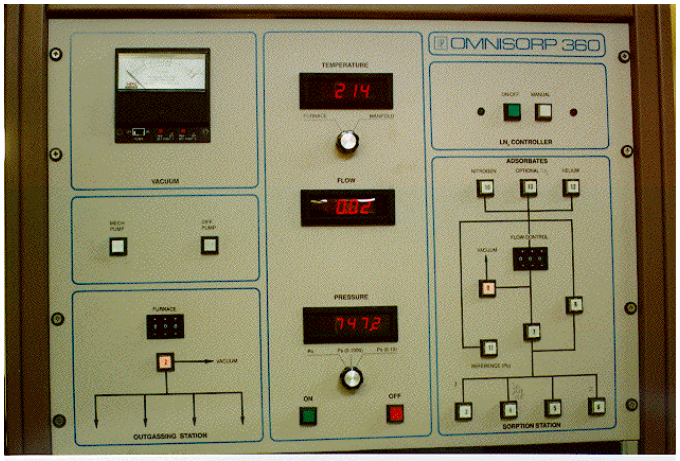

Fig. 2.1 Commercial Vacuum Manifold

In my work, by synthesizing the surfactant-free polystyrene nanoparticle I demonstrate that narrowly distributed polystyrene nanoparticles can be chemically bonded into three-dimension nanoparticle network. Using gel nanoparticles as building blocks to construct gel nanoparticle networks has created new kinds of gel materials that possess properties of both bulk gels and microgel spheres[11]. The same principle can be applied to many latex dispersion systems to create materials of different forms like dipoles, films, clusters and bulk materials composed of polymer latex particles. Two main steps are involved: to synthesize latex particles containing surface functional groups for further crosslinking and to use suitable cross-linking agent to chemically bond the latex particles.

2.3 EXPERIMENTAL

2.3.1 Preparation of Polystyrene Latex

Surfactant-free polystyrene latex particles were synthesized using traditional surfactant-free emulsion polymerization, namely, 3.00g styrene and 0.10g vinyl acetate as monomers (molar ratio of vinyl acetate to styrene of 4.0%), 0.077g methylene-bis-acrylamide (BIS) as crosslinker were dispersed in 240 ml deionized water by stirring and nitrogen bubbling. After purging the oxygen, 0.078g potassium persulfate (KPS) in 7.8 g water solution was added into 68^0C reaction dispersion to initiate free-radical polymerization. The reaction was maintained at 68^0C under nitrogen atmosphere for 10Hrs. The resultant dispersion is milky white and the particle sizes (average hydrodynamic radius, < Rh>, of 83nm) are very narrowly distributed as shown in Fig. 2.2. Compared with previous results of synthesis of pure polystyrene latex particles, adding 4% molar ratio of vinyl acetate did not change the

resultant particle size if only styrene of the same concentration was used. However, the apparent turbidity is lower for PS-PVAc latex dispersion than for PS latex of the same size and the same concentration, inferring the preferential existence of acetate groups on particle surfaces and gradual change in refractive index at latex/water interface. The competitive reaction rate for vinyl acetate is much slower that for that of styrene[12] so that once VAc is reacted, the free-radical chain reaction quickly turns to styrene monomer and acetate groups are expected to be sparsely distributed along the polymer chain networks. The radial distributions of VAc groups can be revealed by neutron scattering.

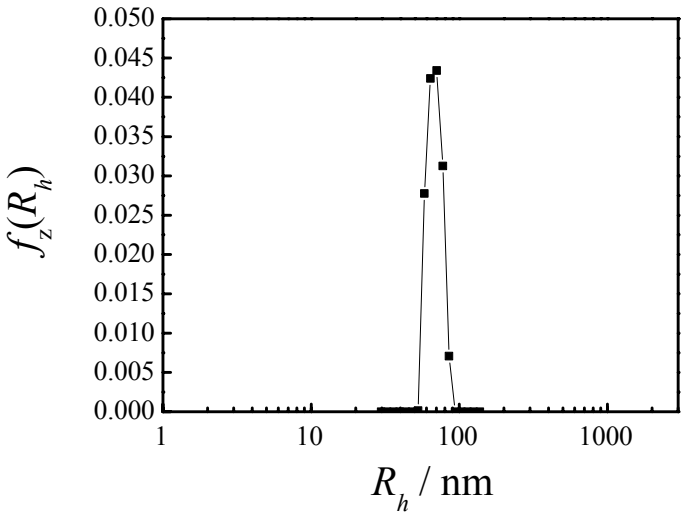

Fig. 2.2 Hydrodynamic radius distribution of Polystyrene latex (R_h = 81nm)

2.3.2 Preparation of Polystyrene Network

The acetate groups were first converted into hydroxyl groups by hydrolysis of PS-VAc latex particles in pH = 13 water medium. After hydrolysis at 95^0C for 6 hrs, the resultant PS-PVA (polyvinyl alcohol) dispersion (concentration of 3.5 wt%) was dialyzed in flowing distilled water for one day, followed by evaporation concentration of the PS-PVA dispersion to solid content of 35 wt%. To crosslink the latex particles, concentrated hydrochloric acid was added into the water dispersion to [H+] ~ 0.4M and an equivalent amount of glutaric dialdehyde was introduced to form co-existed

water/organic phases in equilibrium. Crosslinking was performed at 60^0C for overnight. Cylindrical hard solid latex particle network formed with solid density of 0.5 ~ 0.6 g/cm^3. Thoroughly rinsing with deionized water led to white insoluble PS nanoparticle network sample. On the contrary, dry uncrosslinked PS-PVA chips can be thoroughly re-dispersed in water, forming turbid latex dispersion. The reaction between aldehyde groups on glutaric dialdehyde and hydroxyl groups on PS latex particle surface is nucleophilic addition of alcohols to form acetals. It is interested to note that each glutaric dialdehyde contains a pair of aldehyde groups. When one of them is used for crosslinking a pair of PS latex particles, the other one can either keep unreacted, or chemically bond the same pair of particles, or bonds a pair of alcohol groups on one of the pair of particles. It is unlikely that the other aldehyde bonds another pair of particles because steric repulsion of the huge particles. Consider the huge size of the particles in comparison with small molecules, a pair of particles could be chemically bonded together by many crosslinking molecules.

2.4 RESULTS AND DISCUSSION

2.4.1 Scanning Electronic Microscopy of Polystyrene Network

A schematic figure[13] has been proposed previously showing the gel nanoparticles chemically connect with each other to form three dimensional secondary network, just like small molecules do to form polymer chain network (primary network). This model also suits for polymer latex network. Solid polymer latex is different form gel nanoparticle only in that latex contains no solvent while gel nanparticle does. Fig.2.3 is a SEM picture of PS latex network which is the instrumentational prove of our proposed schematic graph. It shows that PS nanoparticles in their network are in the irregular closely packed state, each nanosphere is connected with two or more other spheres, forming a spatial network. Being chemically bonded, this network bears mechanical strength and hardness. When immersed in toluene, the PS nanoparticle network can swell (the degree of swelling depends on the crosslinking density between the nanospheres), forming gel nanoparticle network.

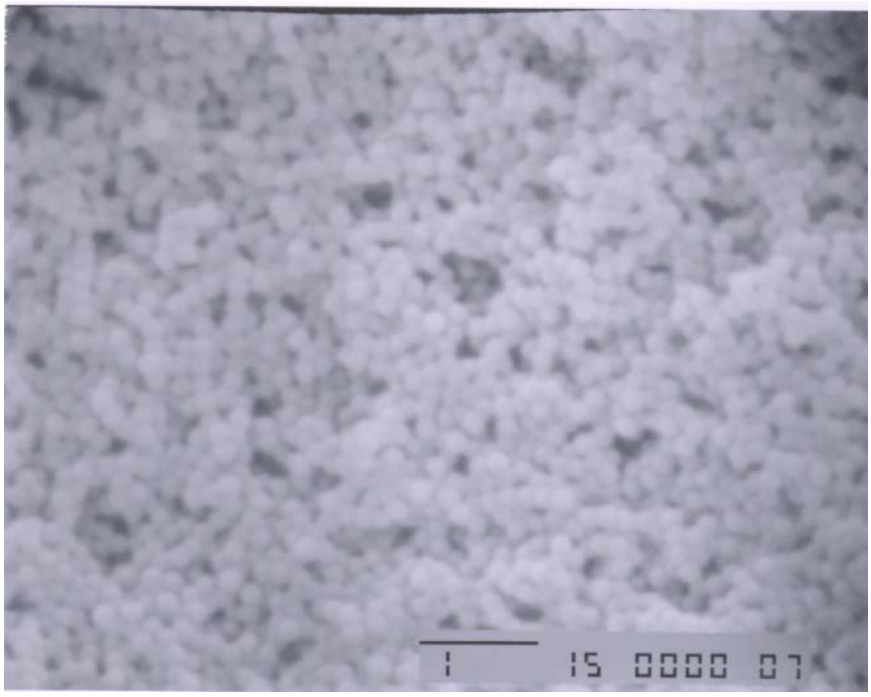

Fig. 2.3 SEM of porous polystyrene

2.4.2 Infrared Spectrum of Polystyrene Network

Infrared spectroscopy was used to give the evidence of chemical crosslinking between PS nanpspheres. Using potassium chloride as matrix, the PS nanoparticle network sample disk was dried overnight in 92^0C to remove all unreacted glutaric dialdehyde. The PS-PVAc sample without further crosslinking was also prepared as comparison using the same preparation procedure. An obvious ester IR absorption peak at ~1742cm^{-1} can be seen before crosslinking (Fig.2.4a), indicating the success of incorporating vinyl acetate with styrene, while after further hydrolysis and crosslinking with glutaric dialdehyde (Fig. 2.4b), the peak disappeared. In Fig.2.4b, however, a new peak of 1723 cm-1 pertaining to aldehyde groups occurred, showing that for most of glutaric dialdehyde molecules only one of the two aldehyde groups was consumed for intra and inter nanoparticle crosslinking, the other remained unreacted because of the steric repulsion, as discussed before. The remained aldehyde groups provide opportunity for further modulation of PS nanoparticle.

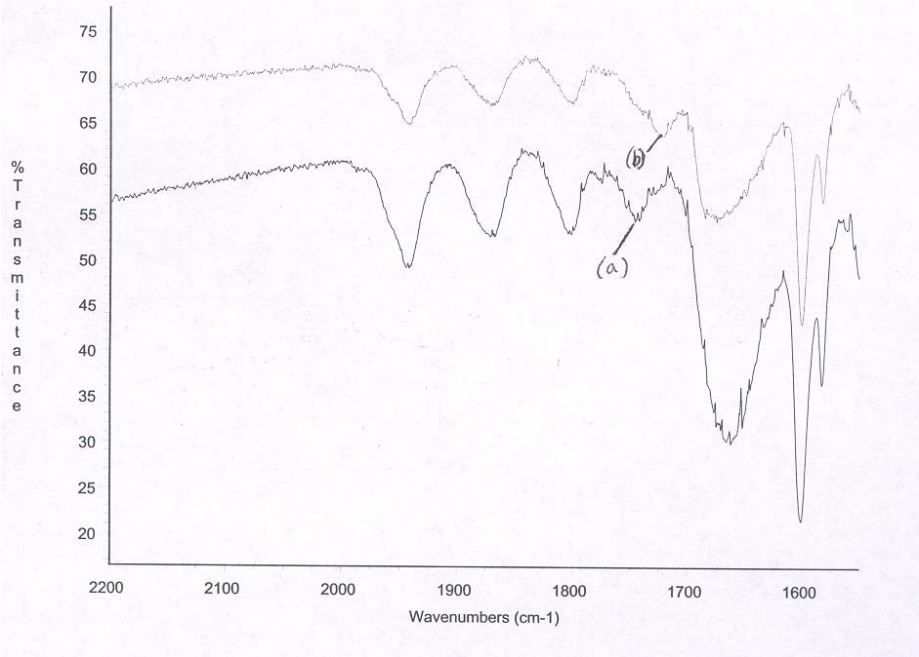

Fig. 2.4 Infrared spectroscopy of polystyrene nanoparticle network (a) before crosslinking (b) after crosslinking

2.4.3 Solubility Experiment

The solubility of pre-crosslinking PS and crosslinked PS was measured. The result (Table 2) shows the particles of PS have been crosslinked.

Table 2 The solubility experiment result

Samples	Solubility in Methylbenzene
PS (before crosslinking)	soluble
PS (after crosslinking)	not soluble

2.4.4 Brunauer-Emmett-Teller (BET) Experiment

As mentioned previously[17], one of the distinct properties of PS nanoparticle network is its abundant penetrated interstices or pores which has the function to absorb/desorption. BET (Brunauer-Emmett-Teller) method was used to characterize the absorption/desorption properties of polystyrene nanonetwork using NOVA 2000 gas adsorption analyzer and nitrogen as adsorbate. Based on two constant BET equation

$$\frac{1}{W((P_0/P)-1)} = \frac{1}{W_m C} + \frac{C-1}{W_m C}\frac{P}{P_0}$$

where W is the weight of gas adsorbed at a relative pressure (P/P_0), W_m is the weight of adsorbate constituting a monolayer of surface coverage, and C is the BET constant related to the energy of adsorption in the first adsorbed layer and hence the indication of magnitude of the adsorbent/adsorbate interactions, W_m and specific area(s) can be obtained from the plot of $[W((P/P_0)-1)]$-1 versus (P/P_0). Fig.ure 2.5 shows BET plot for PS nanoparticle network. The linear fitting with correlation coefficient of 0.997 leads to s = 61m^2/g. While the specific area calculated form s=3/(γρ) for nanosphere with radius γ (83nm) and density ρ (~1g/cm) is 36 m^2/g, a specific area of 61 m^2/g indicates the rough surface of the nanosphere for nitrogen.

The BET result is shown in fig.2.5. From the slope and intercept in fig.2.5, BET constant can be calculated (C = 6.32).

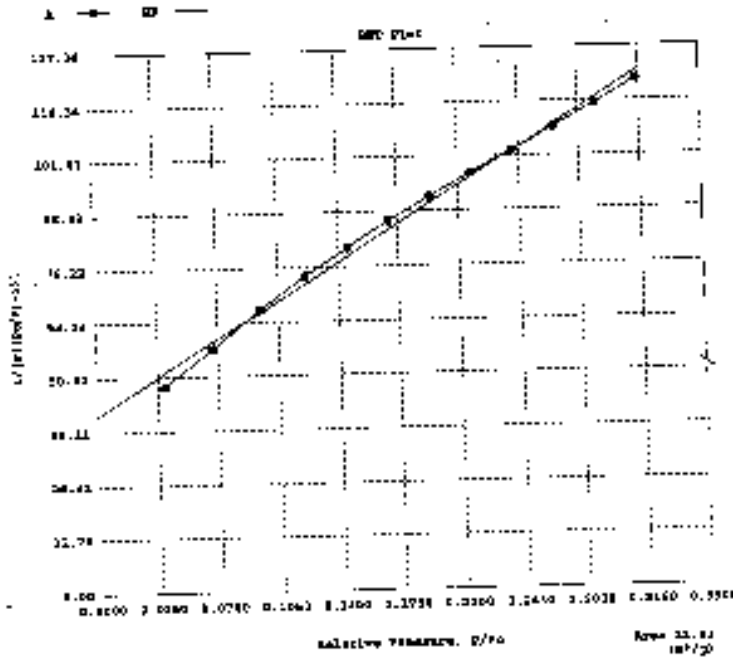

Fig. 2.5 BET plot of polystyrene nanoparticle network : $1/[W(P_0/P-1)]$ vs. relative pressure (P/P_0)

The desorption and isotherm plot are also shown in Fig. 2.6 and Fig. 2.7 respectively. Fig.2.7 shows that no hysteresis happened during the process of adsorption and desorption, ie. adsorption and desorption are reversible.

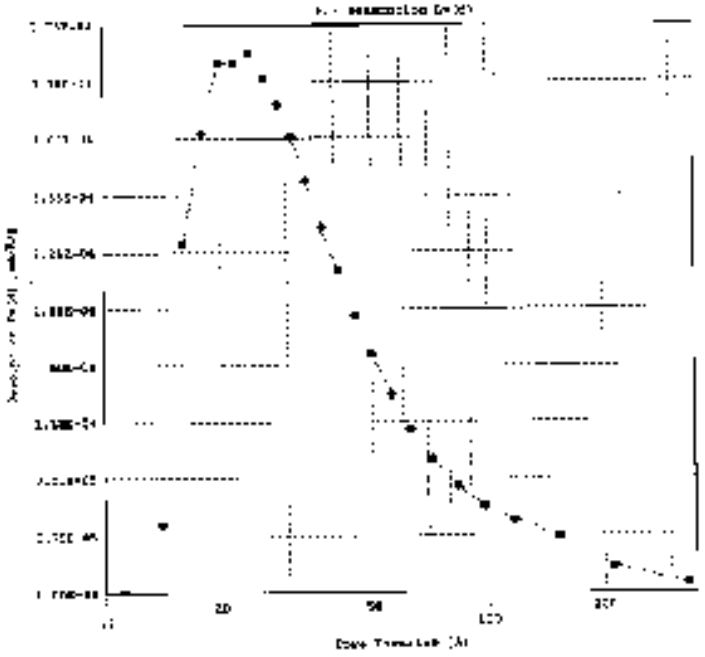

Fig. 2.6 Desorption plot of polystyrene nanoparticle network: desorption Dv vs. pore diameter

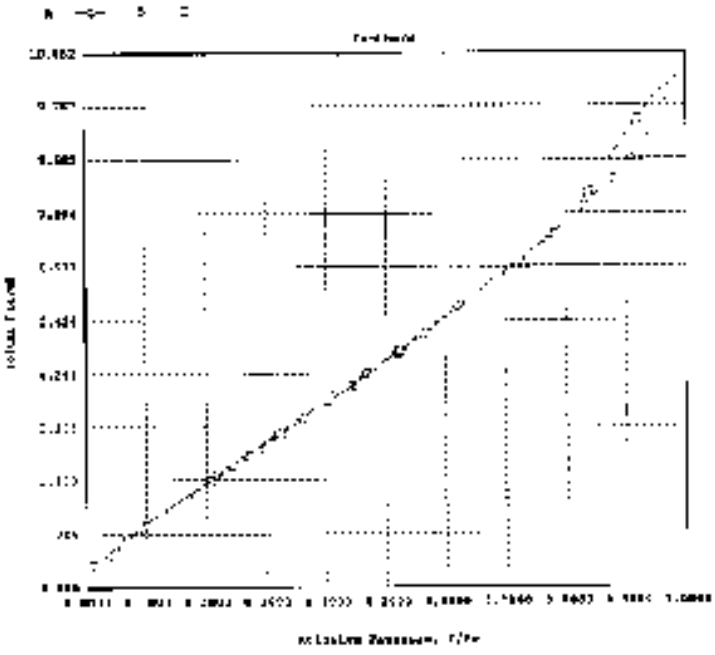

Fig. 2.7 Isotherm Curve: volume vs. relative pressure (A(upper line)-adsorption, B(lower line)-desorption)

2.5 CONCLUSION

Narrowly distributed polystyrene nanoparticle can be chemically bonded into three-dimensional network. Also the particle surface can be modified to possess different functional groups for specific interactions. Thus, the chemically bonded polymer nanoparticle networks will have potential applications as catalysts or used for chromatographic columns.

CHAPTER 2 Reference:

[1] Bangs, L. B. ; Kenny, M. T. Industrial Research, 18, 46, 1976.

[2] Elma E. M. G. Loomans, Tom C. J. Gribnau, Henri P. J. Bloemers and Wim J. G. Schielen Journal of Immunological Methods, Volume 221, Issues 1-2, 131-139, 1998.

[3] Caldwell, K D; Li, J; Li, J T; Dalglesih, D G Journal of Chromatography, Volume 604, Issue 1, 63-71, 1992

[4] Molinabolivar, J. A.; Galisteogonzalez, F.; and Hidalgoalvarez, R. J. Biomaterials Sci. –Polym. Edi. 9, 1103, 1998

[5] Andrianov, A. K.; Payne, L. G. Adv. Drug Delivery Rev. 34, 155, 1998

[6] Michelle S. Kelly and Maria M. Santore, Colloids and Surfaces A: Physicochemical and Engineering Aspects, Volume 96, Issues 1-2, 10,199-215 , 1995

[7] Mats J. Sundell, Esko O. Pajunen, Osmo E. O. Hormi, and Jan H. Nasman Chem. Mater. 5, 372-376, 1993

[8] Q. Ching Wang, Frantlsek Svec, and Jean M. J. Frechet Anal. Chem. 67, 670-674, 1995

[9] O. El-Gholabzouri, M. A. Cabrerizo, R. Hidalgo-Alvarez Journal of Colloid and Interface Science 199, 38-43(1998)

[10] S. Brunauer, "Physical Adsorption" Princeton University Press, Princeton, N. J., 1945.

[11] R.S. Drago, C.E. Webster, and J.M. McGilvray, J. Am. Chem. Soc., 120, 538, 1998

[12] P. Atkins, "Physical Chemistry" Freeman, New York, 1978

[13] I. Langmuir, J. Amer. Chem. Soc., 40, 1361 (1918)

[14] I. Langmuir, J. Amer. Chem. Soc., 54, 2798 (1932)

[15] I. Langmuir, Nobel Lecture, 1932

[16] J. Amer. Chem. Soc., 60, 309 (1938)

[17] Z.B. Hu, X.H. Lu, J. Gao Adv. Mater. 12 No. 16, 1173-1176, 2000